Data Scarcity in Fault Detection for Solar Tracking Systems: the Power of Physics-Informed Artificial Intelligence

Mila Francesca Lüscher[1], Jannik Zgraggen[2], Yuyan Guo[3], Antonio Notaristefano[4], and Lilach Goren Huber[5]

[1,2,5] *Zurich University of Applied Sciences, Technikumstrasse 81, Winterthur Switzerland*
mila.luescher@zhaw.ch
jannik.zgraggen@zhaw.ch
lilach.gorenhuber@zhaw.ch

[2] *Fluence Energy LLC, Hornbachstrasse 50, CH-8008 Zurich, Switzerland*
yuyan.guo@fluenceenergy.com
antonio.notaristefano@fluenceenergy.com

ABSTRACT

Combining physical and domain knowledge in artificial intelligence (AI) models has been gaining attention in various fields and applications. Applications in machine prognostics and health management (PHM) are natural candidates for such hybrid approaches. In particular, they can be efficiently exploited for high fidelity anomaly detection in technical and industrial systems. A natural way for hybridization is using physical models to generate representative data for the training of AI models. Depending on the level of domain knowledge availability, data augmentation can compensate for scarcity of real data from the field. This is particularly attractive for anomaly detection tasks, in which data from the abnormal regimes is limited by definition. On top of this inherent data limitation, many real-world systems suffer from data limitations even within the normal regimes.

In this paper we propose a physics-informed deep learning algorithm for fault detection in grid scale photovoltaic power plants. We focus on a common data scarce scenario that emerges from a low asset monitoring granularity: instead of monitoring the power production of each solar string, the power output is monitored only at combiner-box or even inverter level (monitoring a large number of strings with a single sensor). As a result, the signatures of single local faults can become very subtle and challenging to detect. We show that in this case a physics-informed AI approach significantly outperforms the alternative of a purely data-driven anomaly detection model. This enables high fidelity fault detection in larger solar power plants, that are often limited in the granu-

larity of their condition monitoring data.

1. INTRODUCTION

Utilizing physical information and domain knowledge in conjunction with AI models has become a popular approach to deal with some of the known limitations of AI (Karniadakis et al., 2021), such as the lack of interpretability of AI models and their data-hungry nature. The field of equipment prognostics and health management (PHM) is an ideal application field for such hybrid approaches (Rausch, Goebel, Eklund, & Brunell, 2005; Wu, Sicard, & Gadsden, 2024). For many of the systems, a detailed physical model is already in use for design purposes (Chao, Kulkarni, Goebel, & Fink, 2019; Huber, Palmé, & Chao, 2023), and can be exploited also for PHM. In other systems the fault or degradation mechanisms are well understood and allow for a microscopic or a phenomenological model (Rai & Mitra, 2021; Zgraggen, Guo, Notaristefano, & Goren Huber, 2023).

A typical challenge in PHM tasks is the severe lack of historical failure data. In these cases, the use of physical information to compensate for data scarcity becomes even more attractive than in other application domains. One particularly common approach is to augment the training data using physical models (Frank et al., 2016; Wu et al., 2024). Such models can be used either for operational regimes that are scarce on data (Chao, Kulkarni, Goebel, & Fink, 2022; W. Li et al., 2021), or to directly model fault mechanisms that are rarely seen in operation (Kohtz, Xu, Zheng, & Wang, 2022; Bansal et al., 2022).

In our previous work we took the latter approach (Zgraggen, Guo, Notaristefano, & Goren Huber, 2022). We developed a physical model that corrupts data from a normally operating photovoltaic (PV) plant, thereby generating data with syn-
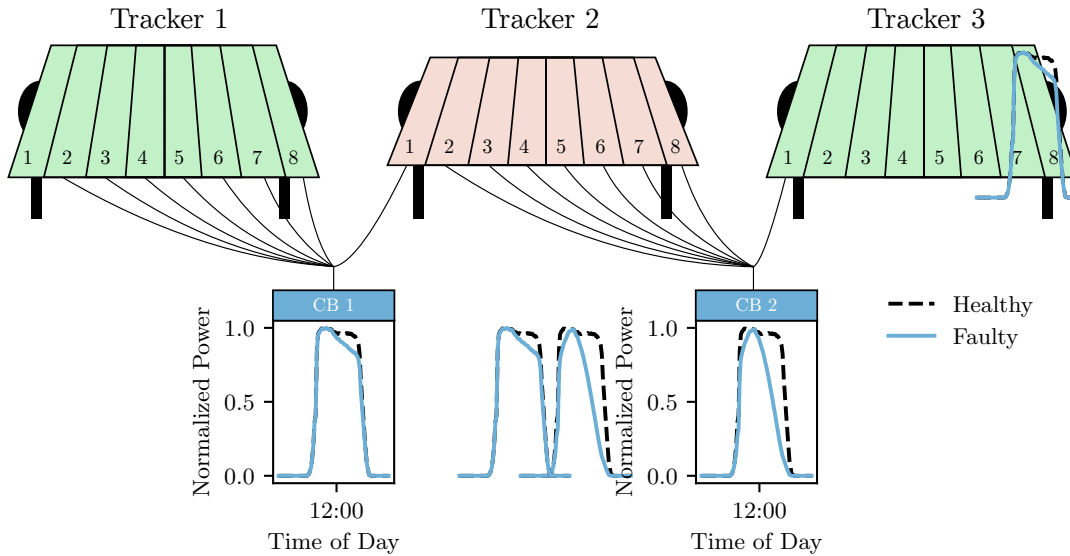
Figure 1. The challenge of low data granularity for tracker fault detection. The eight strings that are mounted on the faulty tracker 2 contribute their power to two different combiner boxes (CBs): CB1 is affected by only one of these strings. Its power profile (bottom left, solid blue) suffers a mild loss compared to the daily reference (dashed black). CB2 is affected by seven of the faulty strings, and suffers a more significant power loss (bottom right).

thetic faults. In this paper we extend this method to allow its applicability under data scarcity in real-world scenarios. The proposed hybrid approach profits from both worlds: on one hand it demonstrates a high ability to mimic the effects of rare faults, without the need for real faults in the data. On the other hand, it does not require a complex physical model of the normal system, as all complex (environmental and operational) effects are already captured by the field data. As opposed to previous approaches to solar plant fault detection, our method is independent of lab data (Chen, Chen, Wu, Cheng, & Lin, 2019; B. Li, Delpha, Diallo, & Migan-Dubois, 2021; Gao & Wai, 2020), simulation data (Chine et al., 2016), or designated data-collecting hardware (Daliento et al., 2017; Amaral, Pires, & Pires, 2021), and was carried out using existing operational data only. Our Physics-Informed Deep Learning (PIDL) approach was shown to perform very accurately with no need for fault data (Zgraggen et al., 2022), and even in a fully unsupervised setting, where the data may be contaminated by unlabeled anomalies (Zgraggen et al., 2023). Moreover, the approach does not require any irradiance measurements, but merely the standard 15-minute measurements of the power output from individual PV strings. Also in this respect our work is rather unique: most of the published work related to PV plant fault detection (Mellit, Tina, & Kalogirou, 2018; Triki-Lahiani, Abdelghani, & Slama-Belkhodja, 2018; Pillai & Rajasekar, 2018; Mansouri, Trabelsi, Nounou, & Nounou, 2021) relies on data at single module or cell resolution, rather than the operationally relevant string-data, often containing dozens or hundreds of modules.

In grid-scale solar power plants, it is often impractical to mon-itor data at string level due to the large number of PV strings involved. As a result, individually monitoring each string often becomes unfeasible. In this case, the output power is monitored and recorded only at a higher spatial granularity level, for example at the level of combiner boxes or even inverters, gathering a large number of strings in a single sensor reading. As shown below, this lower monitoring granularity inevitably leads to a reduced effectiveness in detecting local faults. To the best of our knowledge, there are no previously published studies that address fault detection at combiner-box or inverter level in PV power plants.

In this paper we address the above common scenario of low data granularity by extending our previous PIDL approach. We use a physical model to transfer the method from assets with a high data granularity to assets with a low data granularity. We show that in the case of data scarce assets, the physics-informed (PI) approach is of an even higher benefit compared to purely data-driven anomaly detection.

The contribution of this paper is two-fold. For solar power plant condition monitoring, it offers a high fidelity method to detect anomalous power losses by combining physical knowledge and AI in real-world operational conditions. In a more general context, the paper demonstrates the effectiveness of physics-informed AI for fault detection in data-scarce scenarios, which are common in various application fields. In particular, we show that physical knowledge can be utilized for transfer learning between domains with abundant data and domains with scarce data.

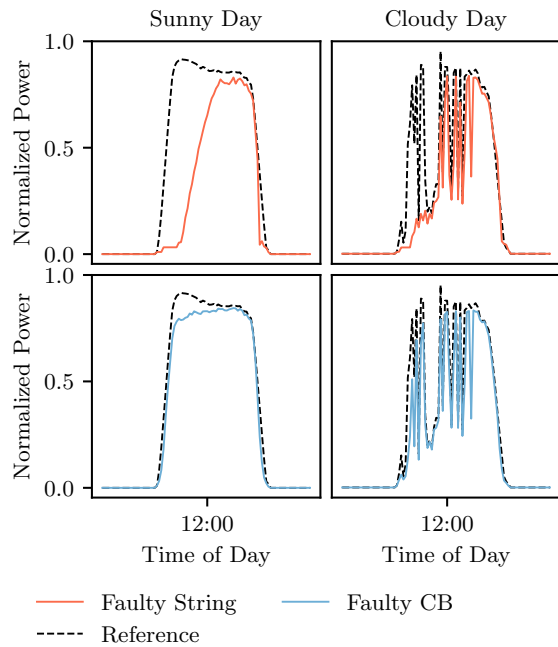In Section 2 we describe the solar tracker use-case on which

Figure 2. The effect of low data granularity on the measured output power. The signature of a real tracker fault on the daily output power of a single string (upper panels) and of the entire combiner box (CB, lower panels). A clear-sky day (left panels) is contrasted with a cloudy day (right panels). The fault signatures are considerably smaller and harder to detect, if only CB-level power data is available.

we demonstrate our approach. In Section 3 we provide the details of the PIDL approach. Finally, the results are shown and discussed in Section 4.

2. DESCRIPTION OF THE USE CASE

The proposed PIDL approach is demonstrated here for the early detection of faults in the tracking system of solar power plants. Solar trackers are rotating units on which PV panels are mounted in order to adjust their orientation during the day according to the position of the sun, thus ensuring maximal power production at any given moment (Racharla & Rajan, 2017). In a common fault mechanism of solar trackers, the trackers get stuck at a certain orientation instead of following the sun. This fault has an immediate implication on the power production, which is significantly reduced compared to the optimum, given certain irradiance and weather conditions. Thus, an automatic early detection of the fault by closely monitoring the power production patterns can significantly reduce the resulting energy losses.

In our previous work (Zgraggen et al., 2022) we developed an algorithm for early detection of tracker faults based on power profiles of PV strings. The algorithm is thus applicable to power plants in which the power production is monitored

for each PV string individually. However, a large fraction of the operational PV power plants nowadays are monitored at a lower granularity, that is, at the level of combiner boxes (CB) or even inverters. In such cases, historical power data is only available for single CBs or inverters, summing up the power of up to tens of individual strings. The single string power is no longer available, thus the previously proposed fault detection algorithm is not directly applicable.

To understand the fault detection challenge posed by the lower data granularity, an example is illustrated in Figure 1, showing two CBs with their related trackers. Since a CB extends over a large area, its strings are typically mounted on several different solar trackers, in this case trackers 1,2 and 3. Thus, if one tracker is faulty, only a fraction of the CB power originates from a string that is affected by the fault while the rest of the strings of this CB do not display any signatures of the tracker fault. In the illustration of Figure 1, Tracker 2 is faulty, while Trackers 1 and 3 are normally functioning. Combiner box CB1 receives its input from 7 strings which are unaffected by the tracker fault (as they are mounted on Tracker 1) and one string which is affected by the fault (as it is mounted on Tracker 2). As a results, the CB power profile (shown at the bottom left in blue) is only mildly impacted by the fault, compared to the reference profile (dashed black). On the other hand, CB2 receives its input from 7 affected strings (mounted on Tracker 2) and only one unaffected string (on Tracker 3). The resulting CB2 power profile (bottom right in blue) shows a much stronger fault signature than the one of CB1. Note that the black dashed profiles are the daily reference power production, calculated from the entire plant data (see explanation in Sec. 3). Moreover, it should be noted that the example is illustrated for a sunny day with clear sky, whereas the effectiveness of the proposed method is shown below under any weather and operational conditions.

As argued above, typical fault signatures on CB power profiles are much more subtle than on string power profiles, and require a higher anomaly detection sensitivity to identify and locate them. Figure 2 demonstrate this effect using data from a real operational PV plant, under different weather conditions. The signatures of a tracker fault on the measured output power are shown at the two monitoring levels: string level vs. CB level. In the upper panels we display (normalized) daily power profiles of a single string which was mounted on a faulty tracker, compared to the daily reference (dashed black). In the lower panels we assume that string level data is unavailable and display the power profiles of the entire CB containing the same string of the upper panels. Since this CB sums up the power of both faulty and intact strings, the signature of the tracker fault is smaller and harder to detect. This is particularly true under cloudy weather conditions, as shown at the right column.

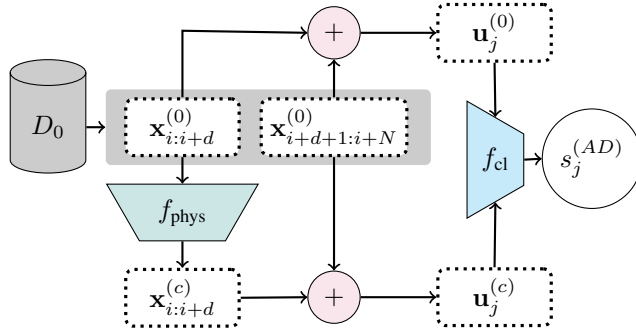The focus of this paper is the transfer of the tracker fault

Figure 3. The proposed Physics-Informed AI fault detection algorithm.

detection algorithm from string level monitoring data to CB level monitoring data, thereby addressing the high fault detection sensitivity challenge.

3. METHOD

In order to achieve high fidelity fault detection of tracker faults for CB-level monitoring data we introduce an extension of our previous string-level PIDL model. The proposed PIDL algorithm for tracker fault detection includes two steps: (i) Data augmentation using a physical model that synthetically generates abnormal power profiles. (ii) Training a binary classifier to distinguish normal from abnormal daily power profiles.

3.1. Physics Informed Data Augmentation

Due to the rare occurrence of tracker faults, real operational power data which is affected by these faults is very scarce. However, data from normal functioning solar power systems is abundant. We exploit this fact, and use operational power data from normally functioning solar plants in order to generate synthetic power profiles under tracker faults. Since the tracker fault mechanism is well understood, we develop physical equations that enable a simple transformation of a healthy power profile into a faulty one. In this way we can simulate diverse fault scenarios and augment the training data with a large number of realistic tracker fault examples. In a second step, the augmented data containing both healthy and faulty power profiles is used to train a binary classifier that distinguishes between normal and abnormal power profiles, thereby enabling identification and localization of tracker faults in large power plants. In the following we describe the physics informed data augmentation method.

A tracker fault affects the power production of the solar strings that are mounted on the faulty tracker. Neighboring strings, if mounted on healthy functioning trackers, remain unaffected. In particular, a common situation (as illustrated in Figure 1) is that out of the N strings that are combined into one CB, only $d < N$ are mounted on a faulty tracker and the rest $N - d$ strings are mounted on healthy trackers.

In order to synthetically generate CB power profiles that correspond to various types of tracker faults, we model d faulty string power profiles that result from a tracker getting stuck at an angle θ_0. This is done using a physical model f_{phys} of the fault mechanism that "corrupts" normal power profiles of single strings, turning them into faulty profiles. The d synthetically generated faulty profiles are added to $N - d$ real healthy string profiles from the operational system, to obtain a synthetic CB profile which is partially affected by a tracker fault, as depicted in Figure 3.

The generation of a faulty string power profile $x^{(c)}(t)$ out of a healthy string profile $x^{(0)}(t)$ is done using the equations

$$x^{(c)}(t) = c_p \left[(1 - \gamma) g(\theta_0, \theta_{\text{i}}^*(t)) + \gamma \right] x^{(0)}(t)$$
$$g(\theta_0, \theta_{\text{i}}^*(t)) = \frac{\cos \theta_0 \cdot f_{\text{IAM}}(\theta_0)}{\cos \theta_{\text{i}}^*(t) \cdot f_{\text{IAM}}(\theta_{\text{i}}^*(t))}. \quad (1)$$

with $f_{\text{IAM}}(\theta_{\text{i}}) = 1 - b_0(1/\cos \theta_{\text{i}} - 1)$ and where $\theta_{\text{i}}^*(t)$ is the optimal tilt angle of the tracker at time t, θ_0 is the stuck angle of the faulty tracker, b_0 and γ are model parameters estimated empirically using the data, by fitting 10 samples of faulty profiles from the operational data of the string-level PV plant (we note that such profiles are only needed for a single plant, and are not required for the target plant at CB level). The parameter c_p is a degradation loss coefficient, assumed to range between 0.8 and 1 in order to simulate slight losses which are unrelated to tracker faults, and may exist also in healthy strings. For details of the physical model we refer the reader to (Zgraggen et al., 2022).

By adding up d faulty and $N - d$ normal string profiles, a synthetically generated faulty CB power profile $u^{(c)}(t)$ obtains the form

$$u^{(c)}(t) = \frac{1}{d} \sum_{i=1}^{d} x_i^{(c)}(\theta_0, \gamma, b_0, c_p; t) + \frac{1}{N - d} \sum_{i=d+1}^{N} x_i^{(0)}(t) \quad (2)$$

where $x_i^{(c)}(\theta_0, \gamma, b_0, c_p; t)$ is the ith corrupted string profile and $x_i^{(0)}(t)$ is the ith healthy string profile. The model parameters θ_0, γ, b_0 and c_p are sampled from uniform distributions within realistic ranges to represent all physically viable configurations (see (Zgraggen et al., 2022) for details), but are kept identical for all of the strings that belong to the same CB. The number of corrupted strings d is drawn randomly from the range $1...N$ in order to cover all possible configurations under the constraint of N strings in one CB (which is given by the plant configuration).

In addition to the generation of faulty CB profiles, we generate an equal amount of healthy CB profiles by simply adding N healthy adjacent string profiles. Note that we follow the modelling approach described in (Zgraggen et al., 2022), in which we randomly introduce mild physics-informed modifications to the healthy profiles in order to mimic the ef-

fects of small power losses that are unrelated to tracker faults. As shown in (Zgraggen et al., 2022), allowing this physics-inspired stochastic variability in the training data, increases both the accuracy and the robustness of the model predictions.

The proposed data augmentation process ensures a large diversity of tracker faults with different intensities, stuck angles and under various soiling or degradation conditions. Moreover, an important advantage of our approach is its mathematical structure, that enables using real operational power profiles and transforming them into faulty profiles by mathematically "injecting" a known fault mechanism into them. As a result, complex features of the model inputs, such as diverse weather effects, are already accounted for, and do not need to be modeled.

We note that the CB-level model described above uses string power profiles to generate CB power profiles. As such, it assumes the availability of normal data from one power plant which is monitored at string level. The results we show below were obtained after training on data from a string-level plant (the source plant), but tested on an operational power plant with CB monitoring only, in a different geographic location (the target plant). With this we demonstrate that effective fault detection is transferable to the target plant without string-level data availability, owing to the physics informed modeling approach.

3.2. CNN fault classifier

The empirical-physical model of the fault mechanism is used to augment the normal data set, such that it now contains healthy as well as faulty power profiles at CB level, $u_j^{(0)}(t)$ and $u_j^{(c)}(t)$ respectively. Each daily profile is a time-series of size 96 (due to a 15 minute resolution of the original sensor data). At a next step, the augmented data set, containing balanced healthy and faulty samples is pre-processed by subtracting from each power profile the daily reference profile, calculated as the 0.9 quantile over the entire plant at any given moment in time (see (Zgraggen et al., 2022) for details). The resulting power deviation profiles are used to train a 1d-CNN classifier f_{cl} that assigns an anomaly score $s_j^{(AD)}$ to each daily profile, as depicted in Figure 3. This allows to detect faulty combiner boxes (thereby locating the related faulty trackers) at the end of each day, which is the relevant time resolution for decision making in practice. The CNN contains three one-dimensional convolutional layers followed by two fully-connected layers, with a total of around 30'000 trainable parameters. The network architecture was optimized using a grid search to tune the number of layers and filters and the learning rate.

We trained the classifier with 700'000 CB power profiles, half of which include synthetic tracker fault effects. All profiles originate from one single PV power plant during a time pe-
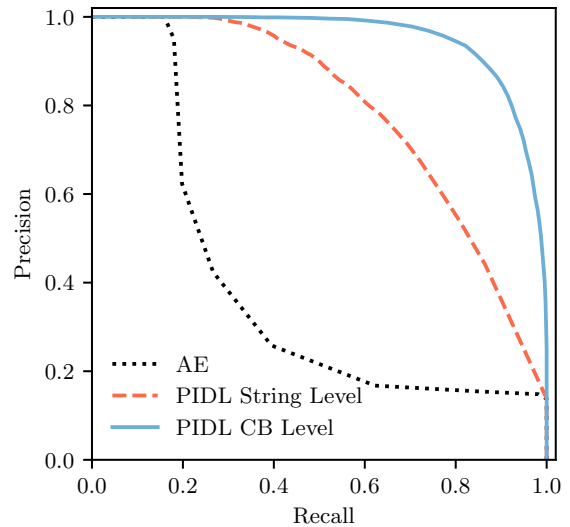

Figure 4. Fault detection evaluation using precision-recall curves. The performance of the proposed CB-level PIDL model (solid blue) is compared with a simpler string-level PIDL (dashed red) and a purely data-driven convolutional AE model (dotted black).

riod of one year. The test data originates from another PV power plant, monitored at CB level, and includes 5349 CB power profiles collected during a time period of two months and containing 857 known faulty profiles, labeled manually by domain experts.

Baselines. We compare the performance of the proposed algorithm with two baseline methods. The first one is a similar PIDL algorithm which is trained using the original string level profiles, rather than CB-level profiles, with and without synthetic faults. This enables us to examine the transferability of the learned features from string to CB level.

The second baseline we compare to is a purely data-driven approach, not making use of any physics-based modeling. In this case we train a convolutional Autoencoder (AE) neural network to reconstruct power profiles. The AE is trained with the normal part of the data only, not including any tracker faults. The normalized reconstruction errors are then used as fault indicators, with a threshold typically set at the tail of the training distribution of reconstruction errors. The feature extraction layers of the AE are four 1d-convolutional layers, similarly to the PIDL network described above, with a similar number of 46'000 trainable parameters.

4. RESULTS

The performance of the proposed PIDL classifier is evaluated in Figure 4 using a precision-recall curve (PRC). The PRC of the CB-level PIDL method is shown in solid blue, and is
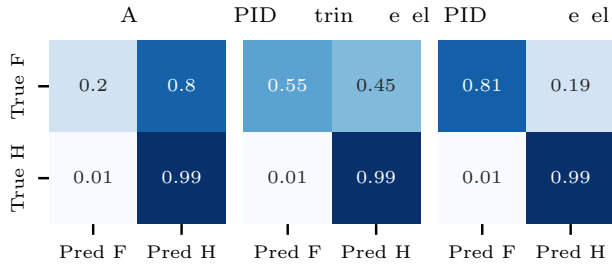
Figure 5. Fault detection evaluation using confusion matrices. The performance of the proposed CB-level PIDL model (right) is compared to the ones of a string-level PIDL (middle) and a purely data-driven AE (left). For all 3 models, the detection thresholds were set to yield a false positive rate of 1%.

contrasted with the PRC of the string-level PIDL approach (dashed red), and the PRC of the pure data-driven AE model (dotted black). It is evident that a pure data-driven approach does not exploit the physical knowledge of the fault mechanism and thus reaches a much poorer performance than both of the PI approaches. In the case of string-level PIDL, the inputs are not aggregated to mimic CB power profiles whereas in the case of CB-level PIDL the string power profiles are aggregated in various ways such that different tracker fault configurations are simulated in the synthetic data. In this way, also configurations that lead to subtle fault signatures are introduced at training, and can be detected at inference time. As seen from the PRC results, this leads to a significant improvement in the fault detection performance, with an average precision (AP) of 0.95 for the proposed CB-level PIDL, compared to 0.79 for the string-level PIDL. As expected, the purely data-driven AE model is significantly inferior in its fault detection performance, with an AP of 0.38. It should also be noted that the performance of the CB-level PIDL is only slightly worse than the one we reported for the string-level PIDL when tested on string-level data (with an AP of 0.97, see (Zgraggen et al., 2022)).

In addition to the PRC, we compare the fault detection performance using confusion matrices shown in Figure 5. The confusion matrix of the CB-level PIDL model (right) is compared with the ones of the string-level PIDL (middle) and the data-driven AE (left). For the sake of model comparison, all three confusion matrices were generated by selecting a detection threshold that guarantees a low false positive rate of 1%. This is a practically sensible threshold, that reduces the false alarms to a minimum. Fixing the threshold to produce this false positive rate on the test data in all three methods, we obtain a false negative (missed detections) rate of 0.8 with the pure data-driven approach, a rate of 0.45 with the string-level PIDL and a significantly lower rate of 0.19 with the proposed CB-level PIDL algorithm.

The complexity of the fault detection task is demonstrated in Figure 6 using CB power test data from the target power plant. Each panel displays a CB daily power profile (solid blue) compared with the daily reference (dashed black). The upper six panels are examples of CB power profiles with no tracker faults, whereas the six lower panels were labeled as suffering from power losses due to tracker faults. The power profiles in the 6 panels at the left half of the figure were all correctly classified by the proposed PIDL algorithm, as well as by the purely data-driven convolutional AE. Indeed, the fault signatures of the three profiles at the bottom left are rather strong and could be clearly assigned to tracker faults by both models. This stands in contrast to the 6 panels on the right hand side of the figure, which were all correctly classified by the PIDL model, but misclassified by the AE. Here, physical information about the tracker fault mechanism clearly helped to distinguish between true tracker faults (lower panels) and power losses due to other reasons, unrelated to the solar trackers (upper panels). This is despite the fact that such unrelated power losses may be rather high, as seen in the three upper right panels. In all three cases, due to their high power losses compared to the reference, the AE produced high reconstruction errors, leading to false positives. On the other hand, the low power losses of the truly faulty profiles at the bottom right led to missed detections (false negatives) by the AE, because of reconstruction errors that are similar in magnitude to the ones of the training data. Despite their low power losses, and their mild fault signatures, these power profiles were correctly detected as suffering from tracker faults by the CB-level PIDL algorithm.

To conclude, the CB-level PIDL includes a physics-informed data augmentation step that captures important nuances in the fault features, even in case of low data availability that leads to very mild fault signatures. The same data augmentation framework can be easily generalized to any monitoring level, provided the structure of the monitoring data at the operational plant (i.e number of strings per combiner-box or inverter). The only prerequisite is the availability of string level power profiles from a normal functioning power plant that can serve as the baseline for data augmentation. Moreover, one of the advantages of our approach is that it does not require complex measurement and/or modeling of the solar irradiance under various ambient conditions, but relies entirely on a single measured variable: the output power.

The proposed approach of physics-informed data augmentation is generally applicable in systems with some understanding of the fault mechanism. However, we believe that this physical understanding does not need to be complete or to amount to a full microscopic model of the fault mechanism. In many cases, a phenomenological model of the fault signatures on the observed data may be sufficient in order to achieve superior fault detection performance compared to purely data-driven approaches.
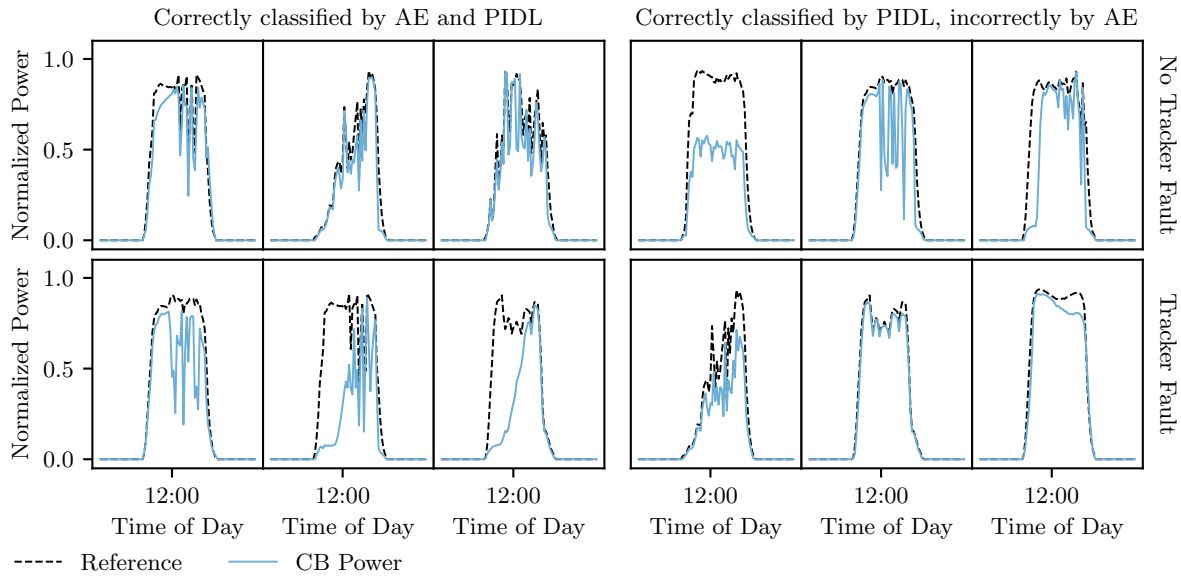
Figure 6. Classification outcomes of the PIDL compared with a purely data-driven AE model. Each panel displays a CB power profile (solid blue) together with the daily reference profile (dashed black). True labeled profiles with tracker faults (bottom row) are contrasted with profiles with no tracker faults (top row). The 6 panels on the left half were correctly classified by both the PIDL and the AE models, whereas the 6 panels on the right were classified correctly only by the proposed PIDL and misclassified by the AE model.

5. CONCLUSIONS

Scarcity of condition monitoring data is a common challenge for practical deployment of fault detection algorithms. Data scarcity may be due to missing data, due to a low time resolution of the data or due to a low spatial resolution. The latter is a common situation in large scale PV power plants, in which condition monitoring data is often available at a low spatial granularity level, e.g. aggregating the monitored power production over a large number of individual assets. However, a similar situation applies to other large infrastructures, where the data volume is often reduced using a more coarse-grained aggregation when monitoring the assets.

In order to enable high fidelity fault detection despite the data scarcity challenge, we introduced a physics-informed artificial intelligence algorithm. With this approach, physical information is exploited in order to transfer the data augmentation from a domain with abundant data to a domain with scarce data. We demonstrated the high performance of the algorithm on operational data from a PV power plant with a low data granularity, and showed its clear superiority over a purely data-driven approach. Moreover, we showed that its performance is similar to our previous results achieved on a high data granularity power plant. Future research directions include an extension of the approach to additional fault and power loss mechanisms, aiming at effective diagnostics of the power loss root cause.

REFERENCES

Amaral, T. G., Pires, V. F., & Pires, A. J. (2021). Fault detection in pv tracking systems using an image processing algorithm based on pca. *Energies*, *14*(21), 7278.

Bansal, P., Zheng, Z., Shao, C., Li, J., Banu, M., Carlson, B. E., & Li, Y. (2022). Physics-informed machine learning assisted uncertainty quantification for the corrosion of dissimilar material joints. *Reliability Engineering & System Safety*, *227*, 108711.

Chao, M. A., Kulkarni, C., Goebel, K., & Fink, O. (2019). Hybrid deep fault detection and isolation: Combining deep neural networks and system performance models. *arXiv preprint arXiv:1908.01529*.

Chao, M. A., Kulkarni, C., Goebel, K., & Fink, O. (2022). Fusing physics-based and deep learning models for prognostics. *Reliability Engineering & System Safety*, *217*, 107961.

Chen, Z., Chen, Y., Wu, L., Cheng, S., & Lin, P. (2019). Deep residual network based fault detection and diagnosis of photovoltaic arrays using current-voltage curves and ambient conditions. *Energy Conversion and Management*, *198*, 111793.

Chine, W., Mellit, A., Lughi, V., Malek, A., Sulligoi, G., & Pavan, A. M. (2016). A novel fault diagnosis technique for photovoltaic systems based on artificial neural networks. *Renewable Energy*, *90*, 501–512.

Daliento, S., Chouder, A., Guerriero, P., Pavan, A. M., Mellit, A., Moeini, R., & Tricoli, P. (2017). Monitoring, diagnosis, and power forecasting for photovoltaic fields: A review. *International Journal of Photoenergy*, *2017*.

Frank, S., Heaney, M., Jin, X., Robertson, J., Cheung, H., Elmore, R., & Henze, G. (2016). *Hybrid model-based and data-driven fault detection and diagnostics for commercial buildings* (Tech. Rep.). National Renewable Energy Lab.(NREL), Golden, CO (United States).

Gao, W., & Wai, R.-J. (2020). A novel fault identification method for photovoltaic array via convolutional neural network and residual gated recurrent unit. *IEEE access*, *8*, 159493–159510.

Huber, L. G., Palmé, T., & Chao, M. A. (2023). Physics-informed machine learning for predictive maintenance: applied use-cases. In *2023 10th ieee swiss conference on data science (sds)* (pp. 66–72).

Karniadakis, G. E., Kevrekidis, I. G., Lu, L., Perdikaris, P., Wang, S., & Yang, L. (2021). Physics-informed machine learning. *Nature Reviews Physics*, *3*(6), 422–440.

Kohtz, S., Xu, Y., Zheng, Z., & Wang, P. (2022). Physics-informed machine learning model for battery state of health prognostics using partial charging segments. *Mechanical Systems and Signal Processing*, *172*, 109002.

Li, B., Delpha, C., Diallo, D., & Migan-Dubois, A. (2021). Application of artificial neural networks to photovoltaic fault detection and diagnosis: A review. *Renewable and Sustainable Energy Reviews*, *138*, 110512.

Li, W., Zhang, J., Ringbeck, F., Jöst, D., Zhang, L., Wei, Z., & Sauer, D. U. (2021). Physics-informed neural networks for electrode-level state estimation in lithium-ion batteries. *Journal of Power Sources*, *506*, 230034.

Mansouri, M., Trabelsi, M., Nounou, H., & Nounou, M. (2021). Deep learning based fault diagnosis of photo-voltaic systems: A comprehensive review and enhancement prospects. *IEEE Access*.

Mellit, A., Tina, G. M., & Kalogirou, S. A. (2018). Fault detection and diagnosis methods for photovoltaic systems: A review. *Renewable and Sustainable Energy Reviews*, *91*, 1–17.

Pillai, D. S., & Rajasekar, N. (2018). A comprehensive review on protection challenges and fault diagnosis in pv systems. *Renewable and Sustainable Energy Reviews*, *91*, 18–40.

Racharla, S., & Rajan, K. (2017). Solar tracking system–a review. *International journal of sustainable engineering*, *10*(2), 72–81.

Rai, A., & Mitra, M. (2021). A hybrid physics-assisted machine-learning-based damage detection using lamb wave. *Sādhanā*, *46*(2), 64.

Rausch, R. T., Goebel, K. F., Eklund, N. H., & Brunell, B. J. (2005). Integrated In-Flight Fault Detection and Accommodation: A Model-Based Study. In *Volume 1: Turbo expo 2005* (pp. 561–569). ASME. doi: 10.1115/GT2005-68300

Triki-Lahiani, A., Abdelghani, A. B.-B., & Slama-Belkhodja, I. (2018). Fault detection and monitoring systems for photovoltaic installations: A review. *Renewable and Sustainable Energy Reviews*, *82*, 2680–2692.

Wu, Y., Sicard, B., & Gadsden, S. A. (2024). A review of physics-informed machine learning methods with applications to condition monitoring and anomaly detection. *arXiv preprint arXiv:2401.11860*.

Zgraggen, J., Guo, Y., Notaristefano, A., & Goren Huber, L. (2022). Physics informed deep learning for tracker fault detection in photovoltaic power plants. In *14th annual conference of the prognostics and health management society, nashville, usa, 1-4 november 2022* (Vol. 14).

Zgraggen, J., Guo, Y., Notaristefano, A., & Goren Huber, L. (2023). Fully unsupervised fault detection in solar power plants using physics-informed deep learning. In *33rd european safety and reliability conference (esrel), southampton, united kingdom, 3-7 september 2023* (pp. 1737–1745).